

To be submitted to *The Astrophysical Journal*

Merging White Dwarf/Black Hole Binaries and Gamma-Ray Bursts

Chris L. Fryer, S. E. Woosley

Lick Observatory, University of California Observatories,
Santa Cruz, CA 95064
cfryer@ucolick.org

Marc Herant

Washington University School of Medicine,
Box 8107, 660 S. Euclid
St. Louis, MO 63110

Melvyn B. Davies

Cambridge Institute for Astronomy,
Madingley Road, Cambridge CH3 0HA¹

ABSTRACT

The merger of compact binaries, especially black holes and neutron stars, is frequently invoked to explain gamma-ray bursts (GRB's). In this paper, we present three dimensional hydrodynamical simulations of the relatively neglected mergers of white dwarfs and black holes. During the merger, the white dwarf is tidally disrupted and sheared into an accretion disk. Nuclear reactions are followed and the energy release is negligible. Peak accretion rates are $\sim 0.05 M_{\odot} \text{ s}^{-1}$ (less for lower mass white dwarfs) lasting for approximately a minute. Many of the disk parameters can be explained by a simple analytic model which we derive and compare to our simulations. This model can be used to predict accretion rates for white dwarf and black hole (or neutron star) masses which are not simulated here. Although the mergers studied here create disks with larger radii, and longer accretion times than those from the merger of double

¹Now at: Astronomy Group, University of Leicester, Leicester LE1 7RH

neutron stars, a larger fraction of the white dwarf’s mass becomes part of the disk. Thus the merger of a white dwarf and a black hole could produce a long duration GRB. The event rate of these mergers may be as high as 10^{-6} yr^{-1} per galaxy.

Subject headings: Gamma-Rays: Bursts, Black Hole Physics, Accretion: Accretion Disks, Stars: White Dwarfs

1. Introduction

As evidence supporting the extra-galactic nature of gamma-ray bursts (GRB’s) mounts (Metzger et al. 1997; Frail et al. 1997), the class of models based on hyper-accreting black holes has become the favorite mechanism for driving these explosions (e.g., Popham, Woosley, & Fryer 1998; Eberl, Ruffert, & Janka 1998). Calculations show that a fraction of the gravitational potential energy released as the material in the disk ($M_{\text{disk}} \approx 0.01 - 2M_{\odot}$) accretes into a small black hole ($M_{\text{BH}} \approx 3 - 10M_{\odot}$) can be converted into a “fireball” which produces the observed gamma-rays (Meszaros & Rees 1992). Such systems form in collapsars or hypernovae (Woosley 1993, 1996; Paczynski 1997) and in the merger of compact binaries consisting of: two neutron stars or a neutron star and a black hole (Paczynski 1991; Narayan, Paczynski, & Piran 1992); a helium star and a black hole (Fryer & Woosley 1998), and, the topic of this paper, a white dwarf and a black hole.

Several mechanisms have been proposed to facilitate the conversion of potential energy into GRB explosion energy. Due to the high densities involved during the merging process, the potential energy may be emitted in the form of neutrinos, and the subsequent annihilation of these neutrinos could power a GRB (Goodman, Dar, & Nussinov 1987). Meszaros & Rees (1992) first pointed out the advantages of disk geometry for enhancing neutrino annihilation. However, unless the accretion rate is very high, over a few hundredths of a solar mass per second, Popham et al. (1998) have shown that neutrino emission is inefficient as the energy released in the disk is advected into the hole. Alternatively, and especially for lower accretion rates and lower disk viscosity, the amplification of magnetic field in the disk can tap either the black hole rotational energy or the potential energy of the accreting material to drive a relativistic jet and create a GRB (Blandford & Znajek 1977; MacDonald et al. 1986; Paczynski 1991, 1997; Woosley 1996; Meszaros & Rees 1997, Katz 1997). However, these magnetically based models are currently not sufficiently accurate to make quantitative predictions (Livio, Ogilvie, & Pringle 1998).

One scenario to form binaries consisting of a black hole and a white dwarf (WD/BH binaries) begins with main-sequence stellar systems having extreme mass ratios ($M_{\text{primary}} \gtrsim 30M_{\odot}$, $M_{\text{secondary}} \approx 1 - 8M_{\odot}$). The formation scenario for white dwarf binaries with neutron star companions is similar, only with a primary star mass between ≈ 8 and $\approx 30M_{\odot}$. As the massive star evolves off the main sequence, a common envelope phase may occur that ejects the primary’s hydrogen envelope. Beyond some critical mass (roughly $30M_{\odot}$), massive stars are thought to form black holes, either by a failed explosion, or through significant fallback (Woosley & Weaver 1995, Fryer 1998). The more massive primary eventually collapses into a $3 - 15M_{\odot}$ black hole and forms a binary consisting of a black hole and a main-sequence star. As the secondary expands and the orbit shrinks, a second mass transfer phase commences. This phase is observed in the closest of these systems as a low-mass X-ray binary (e.g. J0422+32-Nova Per, 2023+338 Nova Cyg). Roughly 20 binary systems with a black hole and a low-mass companion have been observed and many, as yet undetected systems may exist (see Tanaka & Shibazaki, 1996, for a review). These systems generally involve main-sequence secondaries that lose a significant amount of their mass while still burning hydrogen and do not evolve into massive ($> 0.5M_{\odot}$) white dwarfs. However, slightly wider binaries do not undergo mass transfer until after the secondary has evolved off the main sequence and produce the systems which we model in this paper. Unfortunately, the formation rate of the observed low mass X-ray binaries is difficult to determine, and estimating the number of wider systems from observations is impossible. It is these more massive companions that dominate the merging WD/BH binaries and hence, the typical merging system consists of a black hole and massive ($\gtrsim 0.9M_{\odot}$) white dwarf.

An alternative evolution scenario for WD/BH binaries begins with less extreme mass ratios in a system where the primary initially forms a neutron star in a supernova explosion. As the secondary expands off the main-sequence and a common envelope phase ensues, the neutron star accretes rapidly via neutrino emission (allowing the accretion rate to greatly exceed the photon Eddington limit) and eventually collapses to a low mass black hole (see Fryer, Benz, & Herant 1996, Bethe & Brown 1998). Because this common envelope phase happens quickly, it is unlikely that systems evolving through this scenario will be observed, and no merger rate can be predicted from the observations.

Unfortunately, uncertainties in black hole formation and binary evolution also make it difficult to make any firm predictions using population synthesis studies, but the merger rate is likely to lie in the range from $10^{-9} - 10^{-6} \text{ yr}^{-1}$ per Milky-Way like galaxy (Fryer, Woosley, & Hartmann 1999). The large uncertainties in the merger rate are primarily due to uncertainties in the critical mass beyond which massive progenitor stars collapse to black holes and in the kick imparted to black holes.

Black holes and white dwarfs can also merge through collisions in dense star regions such as in galactic centers and globular clusters. Sigurdsson & Rees (1997) predict a neutron star/white dwarf merger rate of $\sim 10^{-7} \text{ yr}^{-1}$ per galaxy. Low mass black holes will merge with white dwarfs roughly at the same rate (or an order of magnitude less) depending upon the black hole formation rate. This rate is comparable to the merger rate predicted by Quinlan & Shapiro (1987, 1989, 1990). Depending on the beaming fraction, this rate is certainly sufficient to give the observed GRB statistics (Wijers et al. 1998), provided, of course, that the merger produces a GRB.

In this paper, we model the merger of black holes and white dwarfs on the computer using a three-dimensional hydrodynamics code based on the Smooth Particle Hydrodynamics (SPH) method (Benz 1990). We follow the merger from the initial Roche-lobe overflow through the complete disruption of the white dwarf into a disk. Roche-lobe overflow for compact objects differs from that for giant stars in several ways: (b) due to the degeneracy of the compact object, its radius increases as it loses mass, and (c) the orbital angular momentum is far from conserved (\equiv the mass transfer is not “conservative”). We discuss this physics, applicable to most compact object mergers, in §2. A description of the code along with a presentation of the simulations, including a comparison to the analytic estimates of §2, is given in §3. We conclude with a discussion of the accretion disks formed in these mergers and their suitability as GRB models.

2. Accretion Disk Formation

Whether or not the accretion disks formed in WD/BH mergers produce the necessary GRB explosion energies is determined by the accretion rate and the angular momentum of those disks, which in turn, depends upon the size and mass of the accretion disk. It is important to know, then, how quickly, and at what radius, the white dwarf is torn up by the gravitational potential of the black hole and transformed into an accretion disk which might fuel a GRB. One might naively assume that, since the white dwarf is less massive than the black hole ($M_{\text{BH}} \sim 3 - 10M_{\odot}$, $M_{\text{WD}} \sim 0.5 - 1.3M_{\odot}$), that stable accretion will occur and the white dwarf will slowly accrete onto the black hole over many orbital periods. However, as we shall discuss in this section, several aspects of physics conspire to destabilize this mass transfer, leading to the rapid transformation of most of the white dwarf into an accretion disk. This was seen in the merger of double white dwarf binaries by Davies, Benz & Hills (1991).

2.1. Gravitational Radiation

Gravitational radiation plays an important role in the merging of double neutron star or black hole/neutron star systems. For these systems, the emission of gravitational waves tightens the binaries on a timescale comparable to those of the hydrodynamical evolution. However, white dwarfs fill their Roche lobes at much wider separations where the gravitational wave merging timescale is 1-100 yr (depending upon the white dwarf and black hole masses). Although gravitational radiation does cause the orbit to tighten sufficiently to drive the white dwarf to fill its Roche lobe in the first place, once Roche-lobe overflow occurs, the mass transfer rate from the white dwarf onto a disk around the black hole is determined by the transfer of angular momentum and the white dwarf mass-radius relationship which drive unstable mass transfer on much shorter timescales (\sim minutes).

2.2. Effects of Degeneracy

One such destabilizing effect is the inverse relationship of the radii of degenerate objects (neutron star, white dwarf) with respect to mass. For a $\Gamma = 5/3$ polytrope approximation of a white dwarf equation of state, this relationship is (Nauenberg 1972):

$$R_{\text{WD}} \approx 10^4 \left(\frac{M_{\text{WD}}}{0.7M_{\odot}} \right)^{-1/3} \left[1 - \left(\frac{M_{\text{WD}}}{M_{\text{CH}}} \right)^{4/3} \right]^{1/2} \left(\frac{\mu_e}{2} \right)^{-5/3} \text{ km} \quad (1)$$

where R_{WD} , M_{WD} , and μ_e are the radius, mass, and mean molecular weight per electron of the white dwarf and $M_{\text{CH}} \approx 1.4$ is the Chandrasekhar mass. Our simulated white dwarfs differ slightly from this simple relation due to deviations from a simple $\Gamma = 5/3$ polytrope (Fig. 1). The radius of the white dwarf and the masses of the white dwarf and black hole determine the orbital separation at which Roche-lobe overflow commences (Eggleton 1983):

$$A_0 = R_{\text{WD}} \frac{0.6q^{2/3} + \ln(1 + q^{1/3})}{0.49q^{2/3}} \quad (2)$$

where $q = M_{\text{WD}}/M_{\text{BH}}$ is the mass ratio (Fig. 1). Stable mass transfer would require that as the white dwarf loses mass, its orbit widens to place it just at this critical Roche lobe separation. If the white dwarf binary instead remains at a constant orbital separation, the accretion will quickly become unstable as the white dwarf itself expands. This effect is important for all merging systems involving a compact secondary.

2.3. Non-Conservative Mass Transfer

The orbital separation need not remain constant. In conservative mass transfer, when an object accretes onto a more massive companion, orbital angular momentum conservation requires that the orbit expands. However, some fraction of the material can be lost from the system and carry away angular momentum. Hence, although the total angular momentum is conserved, the orbital angular momentum of the binary system decreases, and the orbital separation may actually decrease during mass transfer. This “non-conservative” mass-transfer can be parameterized and solved (see Podsiadlowski, Joss, & Hsu 1992 and references therein). In addition, for mergers with black holes or neutron stars, some of the orbital angular momentum is converted to angular momentum of the accretion disk or to spin angular momentum of the black hole. The change of orbital angular momentum (δJ_{orbit}) of the binary is then given by:

$$\delta J_{\text{orbit}} = [j_{\text{ejecta}}(1 - \beta) + j_{\text{disk}}\beta] \delta M_{\text{WD}} \frac{2\pi A^2}{P} \quad (3)$$

where β is the fraction of mass lost by the white dwarf that is accreted by the black hole (or becomes part of the black hole’s accretion disk), j_{ejecta} and j_{disk} are the specific angular momenta (in the rest frame of the black hole) of the ejected material and the material which is either accreted onto the black hole or becomes part of the accretion disk. A and P are the orbital separation and period of the binary system. Following the procedure of Podsiadlowski, Joss, & Hsu (1992), we derive the orbital separation (A) of the binary during mass transfer including the loss of angular momentum to the accretion disk:

$$\frac{A}{A^0} = \frac{M_{\text{WD}} + M_{\text{BH+disk}}}{M_{\text{WD}}^0 + M_{\text{BH}}^0} \left(\frac{M_{\text{WD}}}{M_{\text{WD}}^0} \right)^{C_1} \left(\frac{M_{\text{BH}}}{M_{\text{BH}}^0} \right)^{C_2} \quad (4)$$

where the values of the constants differ only slightly from those derived by Podsiadlowski, Joss, & Hsu (1992):

$$C_1 \equiv 2j_{\text{ejecta}}(1 - \beta) - 2 + 2j_{\text{disk}}\beta \quad (5)$$

$$C_2 \equiv \frac{-2j_{\text{ejecta}}}{\beta}(1 - \beta) - 2 - 2j_{\text{disk}} \quad (6)$$

and

$$M_{\text{BH+disk}} = \beta(M_{\text{WD}}^0 - M_{\text{WD}}) + M_{\text{BH}}^0, \quad (7)$$

and where superscript 0 denotes pre-mass transfer phase values.

In Roche-lobe overflow onto compact objects (neutron stars or black holes), much of the angular momentum is placed into a disk around that compact object. For the merger of binaries consisting of a black hole and a neutron star, roughly half of the orbital angular

momentum is fed directly into spinning up the black hole (Eberl, Ruffert, & Janka 1998). For wider Roche-lobe overflow systems (e.g. white dwarf mergers) much of the orbital angular momentum is converted into disk angular momentum. (see Papaloizou & Lin 1995 for a review). In systems where the mass transfer is stable and the primary, disk and secondary coexist for many orbital periods, the angular momentum of the disk can be transferred back to the orbital angular momentum of the binary. However, for the runaway accretion caused by the expansion of the white dwarf, the white dwarf is disrupted quickly (2-3 orbital periods) and the torques between the disk and the binary stars are unable to convert the disk angular momentum back to that of the orbit before the disruption of the white dwarf.

Figure 2 shows the orbital evolution for 0.7 and 1.1 M_{\odot} white dwarfs merging with a 3 M_{\odot} black hole for a range of values of j_{disk} (in terms of the white dwarf specific angular momentum $\equiv j_{\text{WD}}$) and assuming no mass is ejected from the system ($\beta = 1$). The critical separation for Roche lobe overflow, shown in Figure 2, marks the dividing line between stable and unstable mass accretion. If the orbit widens faster than the white dwarf expands, the accretion rate onto the black hole is limited to the gravitational wave timescale (1-100 yr) and the merger occurs on these timescales. However, if $j_{\text{disk}} > 0.3, 0.1j_{\text{WD}}$ for 0.7, 1.1 M_{\odot} white dwarfs respectively, the mass transfer is unstable. If the accreting material transports all of its angular momentum to the accretion disk, then the angular momentum of the disk is roughly the angular momentum of the material at the Lagrange point. Assuming tidal locking, for the binary systems we model, this angular momentum is roughly: $j_{\text{disk}} \approx (A - R_{\text{WD}})^2/A^2 j_{\text{WD}} \sim 0.5j_{\text{WD}}$ where A is the orbital separation, R_{WD} is the white dwarf radius, and j_{WD} is the specific angular momentum of the white dwarf in the rest frame of the black hole ($\sim 10^{18} \text{cm}^2 \text{s}^{-1}$). For these high values of j_{disk} , unstable mass transfer is inevitable, and we expect the white dwarf to be tidally disrupted rapidly. But to accurately calculate the mass transfer, and ultimately, the mass accretion rate onto the black hole, we must resort to numerical simulations.

3. Simulations

For our simulations, we use a three dimensional SPH code (Davies, Benz, & Hills 1991) with 6000-16000 particles. We employ the equation of state developed by Lattimer & Swesty (1991) for densities above 10^{11}g cm^{-3} and, for low densities, the equation of state by Blinnikov, Dunina-Barkovskaya & Nadyozhin (1996). We include a nuclear burning network for temperatures above $4 \times 10^8 \text{K}$ (Woosley 1986), though we find that burning is not important, except well within the accretion disk. As we are concerned with the tidal

disruption of the white dwarf and not the accretion of matter in the disk formed from this disruption, we model the black hole (or neutron star) as a point mass and remove particles that fall within $2 - 3 \times 10^8$ cm of the black hole, well before general relativistic effects are important. Similarly, since we are not following the evolution of the accretion disk, the the numerically determined artificial viscosity should not impact our results. However, as a check, we have varied the artificial viscosity by an order of magnitude and find it does not effect the radius at which the white dwarf is disrupted or the initial structure of the accretion disk formed by this disruption. On the other hand, the true physical viscosity does affect the rate at which material is accreted onto the black hole, and hence the pair fireball energy, which we discuss in §4.

With this code, we modeled the tidal disruption of 4 binary systems consisting of a white dwarf (with masses of $0.7, 1.1 M_{\odot}$) and a black hole (with masses of $3, 10 M_{\odot}$) and one system consisting of a $1.1 M_{\odot}$ white dwarf and a $1.4 M_{\odot}$ neutron star. We followed the evolution from the initial Roche-lobe overflow through the destruction of the white dwarf and the formation of an accretion disk (Figs. 3, 4). We assume that gravitational radiation has brought the white dwarf close enough to its black hole companion to overflow its Roche-lobe and transfer mass onto the black hole. We estimate this critical separation using eq. (2). By increasing the separation by 20-30%, we see that no mass transfer takes place (Fig. 3), assuring that our initial separation is within 30% of the actual Roche-lobe overflow separation. We will come back to this error estimate in our discussion of the accretion disk properties at the end of this section.

Before we discuss the disk properties, let us first validate our physical picture of the tidal disruption process. From §2, we expect the specific angular momentum of the disk (in the rest frame of the black hole) to be initially $\sim 0.5j_{\text{WD}}$ and then rise as more of the white dwarf it disrupted. The angular momentum of the simulated disk is $\sim 0.6j_{\text{WD}}$ and then increases to $1.0j_{\text{WD}}$ as the white dwarf is disrupted (Fig. 5). Physically, this means that as the white dwarf transfers mass onto a disk around the black hole, the angular momentum of matter at the Lagrange point is first added to the disk. When the white dwarf is finally disrupted, nearly all of its angular momentum is immediately put into the disk, and the average disk angular momentum equals the initial white dwarf angular momentum. The disk must then shed this angular momentum before this material can accrete onto the black hole (see §4).

Because much of the orbital angular momentum is converted into disk angular momentum, the orbital separation does not expand as one might expect in conservative mass-transfer, and the white dwarf is quickly disrupted by tidal forces. As the black hole accretes mass, the orbital separation of the white dwarf/black hole binary is described

by equation (4). Using equation (4) and assuming no mass is ejected from the system (very little mass is ejected in our simulations, see Figs. 3, 4), we can plot data from the simulations along with the derived separations for a range j_{disk} values (Fig. 6). The remarkable agreement of the best fit of j_{disk} using equation (4) and the actual j_{disk} values from Figure 5 suggests that we have indeed found the relevant physics, and that the orbital separation can be estimated by our simple mass-transfer model.

In these simulations, the mass transfer from the white dwarf becomes increasingly unstable as more of the white dwarf expands beyond its Roche radius and accretes onto a disk around the black hole. Our simulations show that after losing $\sim 0.2M_{\odot}$, the transfer rate becomes so great that the white dwarf is disrupted. This occurs rapidly (in an orbit time), dumping the remains of the white dwarf into an accretion disk around the black hole. This critical mass loss after which the accretion runs away is the one parameter not determined by our analytic model. Using our simulations to constrain this parameter, we are able to describe both the angular momentum and the mass growth rate of the disk from the tidal disruption of the white dwarf.

The specific angular momentum of the disk is given by

$$j \approx \sqrt{GA(M_{\text{BH}} + M_{\text{WD}}^{\text{disruption}})} \quad (8)$$

where G is the gravitational constant, M_{BH} is the black hole mass, and $M_{\text{WD}}^{\text{disruption}} \approx 0.5, 0.8 M_{\odot}$ (for initial white dwarf masses of 0.7, 1.1 M_{\odot} respectively) is the white dwarf mass at the time of disruption taken from our simulations. The orbital separation (A) can be derived from equation (4). The mass transfer rate of the white dwarf onto the disk is roughly

$$\dot{M} = M_{\text{WD}}^{\text{disruption}} / T_{\text{orbit}} \quad (9)$$

where T_{orbit} is the orbital timescale for the binary system after the white dwarf has lost $0.2M_{\odot}$. These results are summarized in Table 1 and the mass-transfer rate can be compared to the simulated rates shown in Figure 7. Note that mass-transfer rates derived from analytical estimates agree within a factor of 2 with those obtained from our simulations. The actual accretion rate onto the black hole is not likely to exceed this mass-transfer rate.

Many of these results rely upon our knowing the exact separation where Roche lobe overflow commences. As we have already mentioned, by increasing the separation by 30%, we find no accretion occurs over many orbits, which suggests that the error in the initial separation is less than 30%. If the errors in the initial orbital separation are less than 30%, our maximum mass-transfer rates are accurate to $\lesssim 30\%$ and the disk angular momenta are accurate to $\lesssim 15\%$. Even changing the initial separation by a factor of 2 only results in a

factor of 3 change in the maximum accretion rate and a change in the angular momenta by less than 40%.

4. Accretion Disk Powered Gamma-Ray Bursts

With these results, we can now address the viability of WD/BH mergers as a GRB model. The mass transfer rate of the white dwarf onto the black hole accretion disk should, in a steady state, balance the accretion rate into the black hole. The actual accretion rate is determined by the efficiency at which the angular momentum is removed from the disk² (Popham, Woosley, & Fryer 1998):

$$\dot{M}_{\text{acc}} \approx 0.37\alpha M_{\text{disk}} M_{\text{BH}}^{1/2} r_{\text{disk},9}^{-3/2} M_{\odot} \text{ s}^{-1}, \quad (10)$$

where α is the standard accretion disk parameter, M_{disk} and M_{BH} are, respectively, the mass of the disk and the black hole in M_{\odot} , and $r_{\text{disk},9}$ is the outer disk radius in 10^9 cm. Figure 8 shows the mass of the disk as a function of radius for our two $M_{\text{BH}} = 3M_{\odot}$ models, from which, given a value of α , we can determine the accretion rate onto the black hole. For values of $\alpha < 0.5$, the accretion rate is limited by the disk accretion and not the mass-transfer rate. Using equation (10), we estimate the effective disk viscosity (α) from accretion rate onto the black hole of our hydrodynamical simulations to be ~ 0.1 .

The energy from neutrino annihilation can be estimated by integrating the following approximate fit to the pair luminosity results of Popham, Woosley, & Fryer (1998):

$$\log L_{\nu,\bar{\nu}}(\text{erg s}^{-1}) \approx 43.6 + 4.89 \log \left(\frac{\dot{M}}{0.01M_{\odot} \text{ s}^{-1}} \right) + 3.4a \quad (11)$$

where $a \equiv J_{\text{BH}}c/GM_{\text{BH}}^2$ is the spin parameter. This fit is reasonably accurate for accretion rates between 0.01 and $0.1M_{\odot} \text{ s}^{-1}$. Table 2 gives the maximum energies for each of our simulations. In the optimistic situation where $\alpha > 0.5$ and the disk accretion rate equals the mass-transfer rate from the white dwarf into a black hole accretion disk, the disruption of a white dwarf around a black hole cannot explain the most energetic gamma-ray bursts without requiring that the mechanism produce strongly beamed jets. Indeed, with isotropic energy requirements as high as 3×10^{53} erg (Kulkarni et al. 1998), the beaming must be extremely high (the burst must be constrained to 0.1% of the sky, that is, the beaming

²This equation applies only when the scale height of the disk is roughly equal to the disk radius. We may be underestimating the viscous timescale by an order of magnitude. However, we are most interested in deriving a lower limit for this timescale (upper limit for the accretion rate).

factor > 1000). However, a wide range of GRB energies may exist, and WD/BH mergers may only constitute a subset of the observations. If $\alpha = 0.1$, the accretion rate drops by about a factor of 5. For the most optimistic mergers of a $1.1M_{\odot}$ white dwarf with a black hole, this lowers the accretion rate on the black hole to $0.01 - 0.02M_{\odot} \text{ s}^{-1}$ and increases the accretion time, causing a net decrease in the total energy produced by neutrino annihilation of roughly 1-2 orders of magnitude. With beaming factors of ~ 100 , WD/BH mergers could still explain bursts with inferred isotropic energies between $10^{48} - 10^{51} \text{ erg}$.

Alternatively, and perhaps more likely for the low-mass accretion rates derived here, the GRB can be powered by the magnetic fields of the disk, which become stretched and amplified as the material accretes. These magnetic fields then extract the rotational energy of the black hole (Blandford & Znajek 1977; MacDonald et al. 1986; Paczynski 1991,1997; Woosley 1993; Katz 1994, 1997; Hartmann & Woosley 1995; Thompson 1996; Meszaros & Rees 1997; Popham et al. 1998). Very roughly, using Blandford-Znajek for example,

$$L_{\text{rot}} = 10^{50} \left(\frac{jc}{GM_{\text{BH}}} \right)^2 \left(\frac{M_{\text{BH}}}{3M_{\odot}} \right)^2 \left(\frac{B}{10^{15} \text{ Gauss}} \right)^2 \text{ erg s}^{-1} \quad (12)$$

where j is the specific angular momentum of the black hole and B is the magnetic field strength in the disk. Table 2 lists the total energy that an initially non-rotating black hole would emit over its accretion timescale assuming the magnetic field energy is 10% of the equipartition energy, or $0.1\rho v^2$. These high magnetic fields are reasonable if the disk viscosity depends upon the magnetic field strength. In this case, the viscosity is initially ~ 0 allowing the disk to continue winding the magnetic field until a sufficiently strong equipartition field is generated, thereby increasing the viscosity and allowing the disk to accrete.

A successful GRB explosion must also avoid excessive baryonic contamination. The disruption of the white dwarf forms a hot thick disk around the black hole (Figure 9), with some of the matter along the angular momentum axis above the black hole (Table 2). The explosion will force its way along this polar region, sweeping up this material (and possibly pushing some aside). Assuming all of the material is swept along with the burst, we can estimate a lower limit for the Lorentz factors (Table 2). Beaming factors of at least 100 are required to achieve the high Lorentz factors needed to power a gamma-ray burst. Even assuming that beaming factors of 100 do occur, low mass white dwarfs do not produce enough energy (or high enough Lorentz factors) to power a gamma-ray burst. Thus, there is some critical white dwarf mass (between $0.7 - 1.1M_{\odot}$ depending upon beaming) below which no visible GRB will form. Because of the strong dependence of the GRB luminosity on the Lorentz factor, the transition from observed gamma-ray burst to non-detectable explosion is sharp. Those explosions that do not achieve the high Lorentz factors will only

be observable in our own Galaxy, and, given the low event rate, will not be detected. We reiterate, however, that most of the merging white dwarfs will be massive (Fryer, Woosley, & Hartmann 1999) and a large fraction of the merging systems may become GRBs.

The merger of a black hole and a massive white dwarf can produce the energies ($10^{48} - 10^{51}$ erg) and the high Lorentz factors to explain the long duration GRBs if the bursts themselves are highly beamed (beaming factors > 100). Assuming the GRB rate for isotropic bursts is 10^{-7} yr^{-1} per galaxy of roughly the Milky Way's size (Wijers et al. 1998), the merger rate of massive white dwarfs and black holes with beaming factors > 10 must be $\gtrsim 10^{-6} \text{ yr}^{-1}$ per galaxy, within the uncertainties of the predicted rates (see §1).

From these results, one might conclude that mergers of white dwarfs and black holes are not likely to play a major role in the production of gamma-ray bursts. However, our estimates of the energy released via magnetic fields are very uncertain. Some magnetic field mechanisms may convert a large fraction of the potential energy of the accreting material into burst energy. If a magnetic field mechanism can be constructed which converts 10% of the potential energy into burst energy, WD/BH mergers would have energies in excess of 10^{52} erg. With beaming into 10gamma-ray bursts.

The merger of a neutron star and a white dwarf is a different story. At these accretion rates, Popham, Woosley, & Fryer (1998) found that much of the energy is advected into the black hole. The hard surface of the neutron star acts as a plug, stopping up this accretion. Unless the neutron star mass quickly exceeds the upper neutron star mass limit, causing it to collapse to a black hole and removing this plug, the accreting material will flow around the neutron star, building up a spherically symmetric atmosphere. Any explosion from the surface will be baryon rich with velocities much less than the speed of light (Fryer, Benz, & Herant 1994). These outbursts will be too dim to observe beyond our Galaxy, and are too rare to observe within our Galaxy.

This research has been supported by NASA (NAG5-2843 and MIT SC A292701), and the NSF (AST-97-31569). We would like to thank Bob Popham, Thomas Janka, and William Lee for many useful corrections and comments. We acknowledge many helpful conversations and communications on the subject of gamma-ray bursts with Andrew MacFadyen, Dieter Hartmann, Max Ruffert, Jonathon Katz and we thank Aimee Hungerford for helpful comments on the manuscript.

REFERENCES

- Benz, W., 1990, in Numerical Modeling of Nonlinear Stellar Pulsations: Problems and Prospects, ed. J.R. Buchler (Dordrecht: Kluwer), 269
- Blandford, R.D., & Znajek, R.L., 1977, MNRAS, 179, 433
- Blinnikov, S.I., Dunina-Barkovskaya, N.V., & Nadyozhin, D.K., 1996, ApJS, 106, 171
- Davies, M.B., Benz, W., & Hills, J.G., 1991, ApJ, 381, 449
- Eberl, T., Ruffert, M., & Janka, H.-Th. 1998, A&A, in preparation
- Eggleton, P.P., 1983, ApJ, 268,368
- Frail, D.A., Kulkarni, S.R., Nicastro, S.R., Feroci, M., & Taylor, G.B, Nature, 389, 261
- Fryer, C.L., Benz, W., Herant, M., 1996, ApJ, 460, 801
- Fryer, C.L., & Woosley, S.E., 1998, 502, L9
- Fryer, C.L., 1998, proceedings of the 2nd International Workshop on Laboratory Astrophysics with Intense Lasers, to appear in ApJ supplements, ed. Remington
- Fryer, C.L., Woosley, S.E., & Hartmann, D., 1999, in preparation
- Goodman, J., Dar, A., & Nussinov, S., 1987, ApJ, 314, L7
- Hartmann, D.H., & Woosley, S.E., 1995, Advances in Space Research, vol. 15, no. 5, 143
- Janka, H.-T., 1991, A&A, 244, 378
- Katz, J.I., 1994, ApJ, 422, 248
- Katz, J.I., 1997, ApJ, 490, 633
- Kulkarni, S.R., Frail, D.A., Wieringa, M.H, Ekers, R.D., Sadler, E.M., Wark, R.M., Higdon, J.L., Phinney, E.S., & Bloom, J.S. submitted to Nature 1998
- Lattimer, J.M., & Swesty, F.D. 1991, Nuc. Phys. A, 535,331
- Livio, M., Ogilvie, I., & Pringle, J.E., 1998, submitted to ApJ

- MacDonald, D.A., Thorne, K.S., Price, R.H., & Zhang, X.-H., 1986, in “Black Holes, the Membrane Paradigm”, Eds. Thorne, K.S., Price, R.H., & MacDonald, D.A., Yale Univ. Press
- Meszaros, P., & Rees, M. J., ApJ, 1992, 397, 570
- Meszaros, P., & Rees, M. J., 1997, 482, L29
- Metzger, M.R., Djorgovski, S.G, Kulkarni, S.R., Steidel, C.C., Adelberger, K.L., Frail, D.A., Costa, E., & Frontera, F., 1997, Nature, 387, 389
- Narayan, R., Paczyński, B., & Piran, T. 1992, ApJ, 395,L83
- Nauenberg, M., 1972, ApJ, 175, 417
- Paczynski, B., 1991, AcA, 41, 257
- Paczynski, B., 1997, ApJ, 484, L45
- Papaloizou, J.C.B., & Lin, D.N.C., 1995, ARA&A, 33, 505
- Podsiadlowski, P., Joss, P.C., & Hsu, J.J.L., 1992, ApJ, 391, 246
- Popham, B., & Woosley, S.E., & Fryer 1998, submitted to ApJ
- Quinlan, G.D., & Shapiro, S.L., 1987, ApJ, 321, 199
- Quinlan, G.D., & Shapiro, S.L., 1989, ApJ, 343, 725
- Quinlan, G.D., & Shapiro, S.L., 1990, ApJ, 356, 483
- Rees, M. J., & Meszaros, P. 1992, MNRAS, 258, 41P
- Ruffert, M., Janka, H.-T., Takahashi, K., Schaefer, G., 1997, A&A, 319, 122
- Sigurdsson, S., & Rees, M.J., 1997, MNRAS, 284, 318
- Tanaka, Y., & Shibazaki, N., 1996, ARA&A, 34, 607
- Thompson, C., 1996, in *Gamma-Ray Bursts: 3rd Huntsville Symposium*, AIP Conf. Proc 384, eds. C. Kouveliotous, M. Briggs, & G. Fishman, AIP:New York, 709
- Wijers, R.A.M.J., Bloom, J., Bagla, J.S., & Natarajan, P., 1998, MNRAS, 294, L13

Woosley, S.E., 1986 Saas-Fee Lecture Notes, 1986, in *Nucleosynthesis and Chemical Evolution*, 16th Advanced Course, Swiss Society of Astrophysics and Astronomy, ed. B. Hauck, A. Maeder, and G. Meynet, Geneva Observatory, 1

Woosley, S.E., 1993, *ApJ*, 405, 273

Woosley, S.E., & Weaver, T.A., 1995, *ApJS*, 101, 181

Woosley, S. E. 1996, in *Gamma-Ray Bursts: 3rd Huntsville Symposium*, AIP Conf. Proc 384, eds. C. Kouveliotous, M. Briggs, & G. Fishman, AIP:New York, 709

Table 1. WD/BH Mergers

Disk Parameters	$M_{\text{WD}} = 0.7$ $M_{\text{BH}} = 10$	$M_{\text{WD}} = 0.7$ $M_{\text{BH}} = 3$	$M_{\text{WD}} = 1.1$ $M_{\text{BH}} = 10$	$M_{\text{WD}} = 1.1$ $M_{\text{BH}} = 3$	$M_{\text{WD}} = 1.1$ $M_{\text{NS}} = 1.4$
$A(10^9 \text{ cm})$	4.98	3.10	2.37	1.49	1.27
$T_{\text{orbit}}(\text{s})$	58.4	48.1	18.9	15.4	12.1
$j_{\text{disk}}(10^{18} \text{ cm}^2 \text{ s}^{-1})$	2.67	1.24	1.87	0.903	0.651
$\dot{M}(M_{\odot} \text{ s}^{-1})$	0.00856	0.01	0.0477	0.0584	0.074
$A^{\text{sim}}(10^9 \text{ cm})^{\text{a}}$	5.0	3.2	2.5	1.6	1.2
$M_{\text{WD}}^{\text{disr}}(M_{\odot})^{\text{b}}$	0.5	0.5	0.8	0.8	0.8
$\dot{M}_{\text{peak}}^{\text{sim}}(M_{\odot} \text{ s}^{-1})^{\text{c}}$	0.012	0.008	0.063	0.079	0.075

^aThe last three rows of data come directly from the simulations, the other rows are derived from the equations in §2,3.

^bThis is the simulated white dwarf mass at the onset of the white dwarf disruption. For our derivations, we assume $M_{\text{WD}}^{\text{disr}} \approx 0.5, 0.8M_{\odot}$ for initial white dwarf masses of 0.7, 1.1 M_{\odot} respectively.

^cThe peak mass-transfer rate from Figure 5.

Table 2. Powering a GRB

Observables	$M_{\text{WD}} = 0.7$	$M_{\text{WD}} = 0.7$	$M_{\text{WD}} = 1.1$	$M_{\text{WD}} = 1.1$
	$M_{\text{BH}} = 10$	$M_{\text{BH}} = 3$	$M_{\text{BH}} = 10$	$M_{\text{BH}} = 3$
$a \equiv jc/GM_{\text{BH}}$	0.21	0.54	0.31	0.69
$E_{\nu,\bar{\nu}}^{\text{max}}(10^{49}\text{Erg})^{\text{a}}$	0.001	0.003	3	50
$E_{\text{rot}}(10^{49}\text{erg})^{\text{b}}$	~ 0.1	~ 1	~ 1	~ 4
$M_{\text{axis}}(M_{\odot})^{\text{c}}$	$10^{-5}(< 10^{-5})$	$10^{-4}(< 10^{-5})$	$10^{-3}(< 10^{-5})$	$10^{-3}(< 10^{-5})$
$(E_{\nu,\bar{\nu}}/M_{\text{axis}}c^2)^{\text{d}}$	$> 5 \times 10^{-4}$	$> 1.5 \times 10^{-3}$	> 2.5	> 25

^a $E_{\nu,\bar{\nu}}^{\text{max}}$ is the neutrino/anti-neutrino annihilation energy released by setting the accretion rate equal to the mass-transfer rate. The luminosity is a function of both the accretion rate and the spin parameter a (see Eq. 9) and we estimate the energy by integrating the luminosity assuming the black hole is not spinning before accretion sets in. The accretion rate can never exceed the mass-transfer rate, and hence, these energies are rough upper limits for the gamma-ray burst energy.

^bWe use the magnetic field estimate of Popham, Woosley, & Fryer (1998) which assumes that the magnetic field energy is 10% of the equipartition energy, or $0.1\rho v^2$.

^cThis corresponds to the mass from the white dwarf which lies along the accretion disk axis and is likely to be swept up in the explosion for a beaming factor of 10(100).

^d $E_{\nu,\bar{\nu}}/M_{\text{axis}}c^2 \approx \gamma$ when $E_{\nu,\bar{\nu}}/M_{\text{axis}}c^2 \gg 1$. We assume beaming factors of 100.

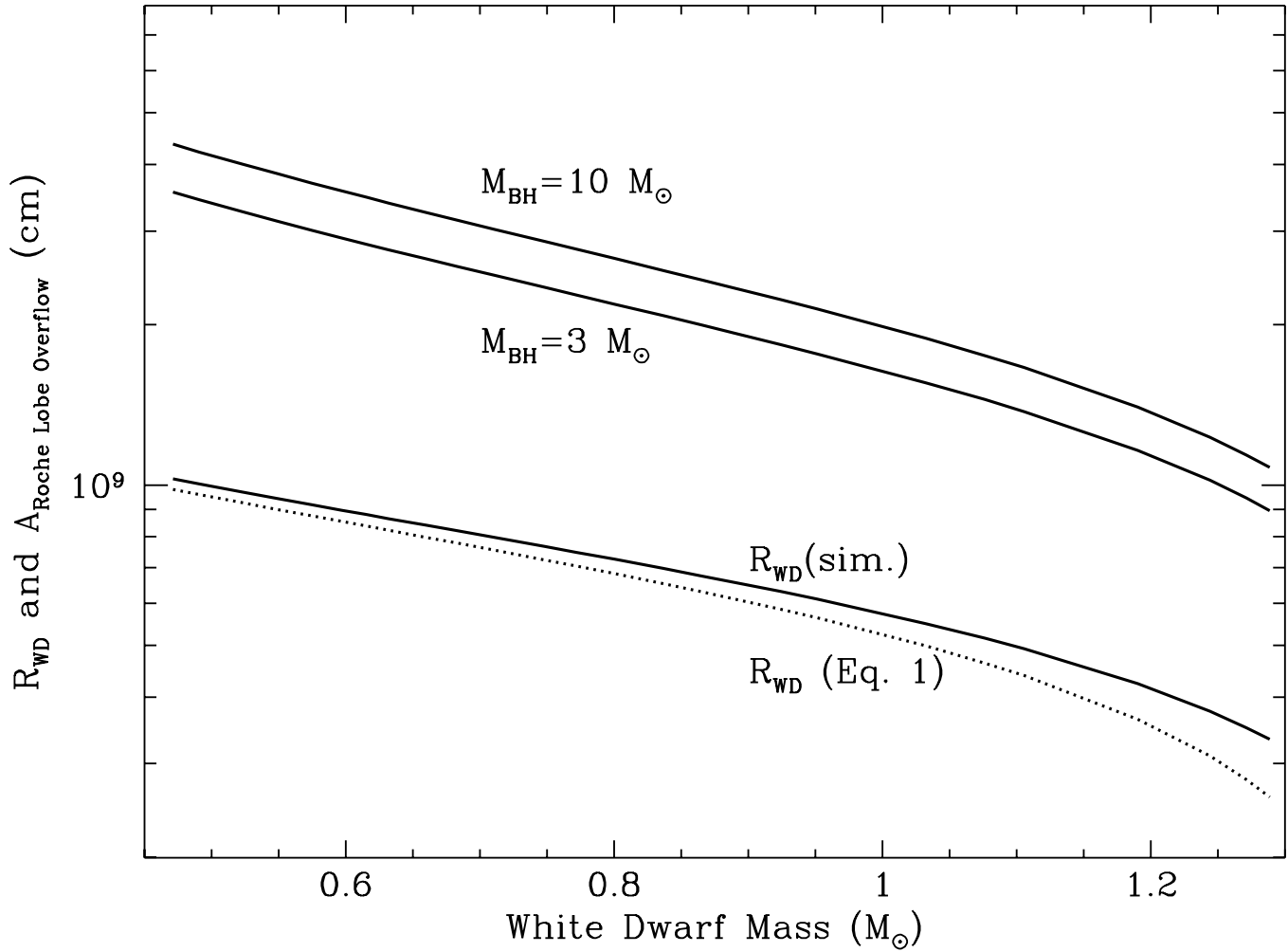


Fig. 1.— White dwarf radii and separations at which Roche-lobe overflow occurs vs. white dwarf mass. The dotted line shows the white dwarf radius using eq. (1) in comparison to our simulated radii. The orbital separations are given for two black hole masses ($3, 10 M_{\odot}$) and demarkate the limit within which the white dwarf overfills its Roche lobe.

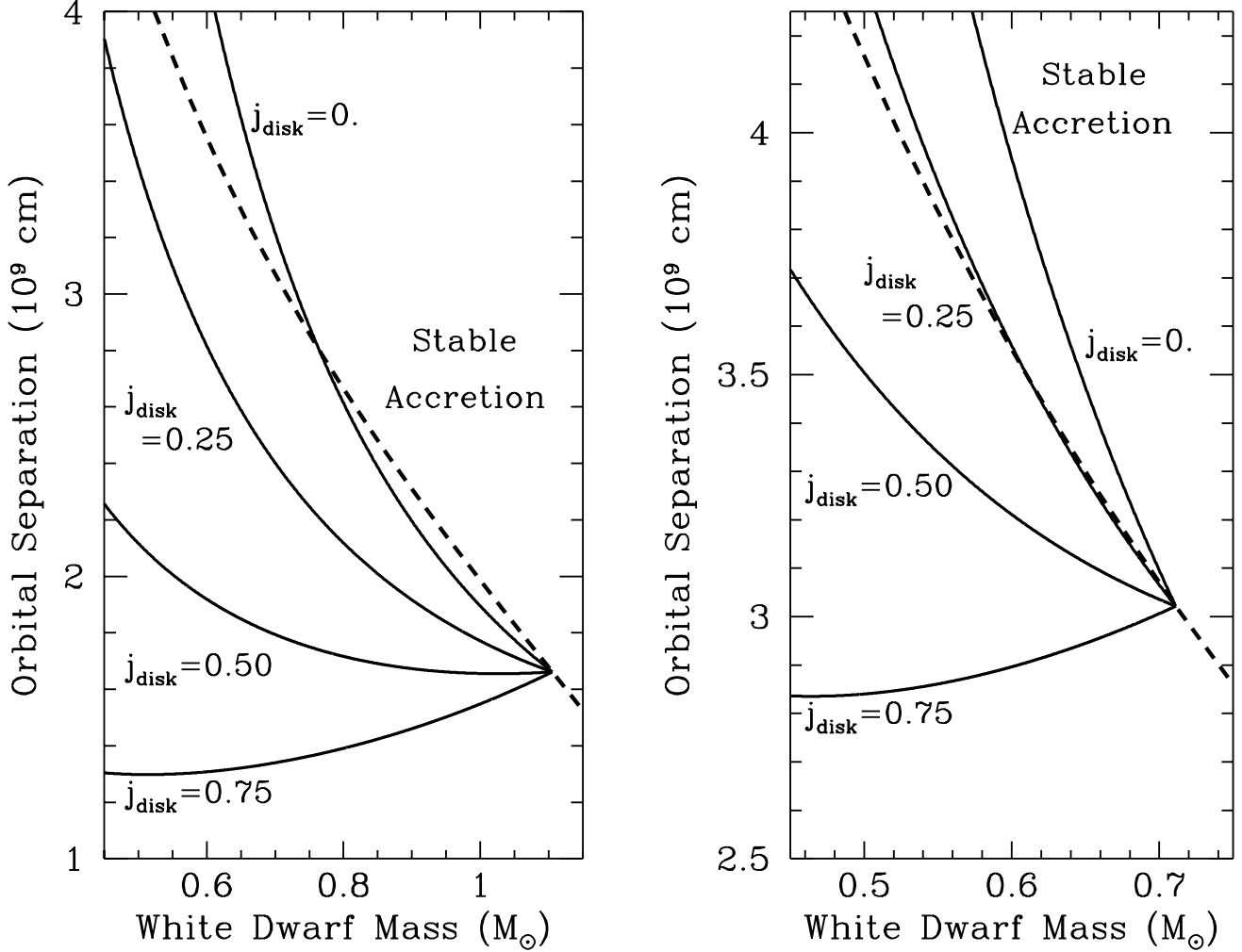


Fig. 2.— Evolutionary paths of the binary separation as a white dwarf accretes onto a $3M_\odot$ black hole for a range of j_{disk} (fraction of specific angular momentum of the the white dwarf) values. The critical Roche-lobe separation is plotted for comparison. If the separation remains above this critical separation, stable accretion occurs. Otherwise, the accretion is unstable and the white dwarf quickly accretes onto the black hole.

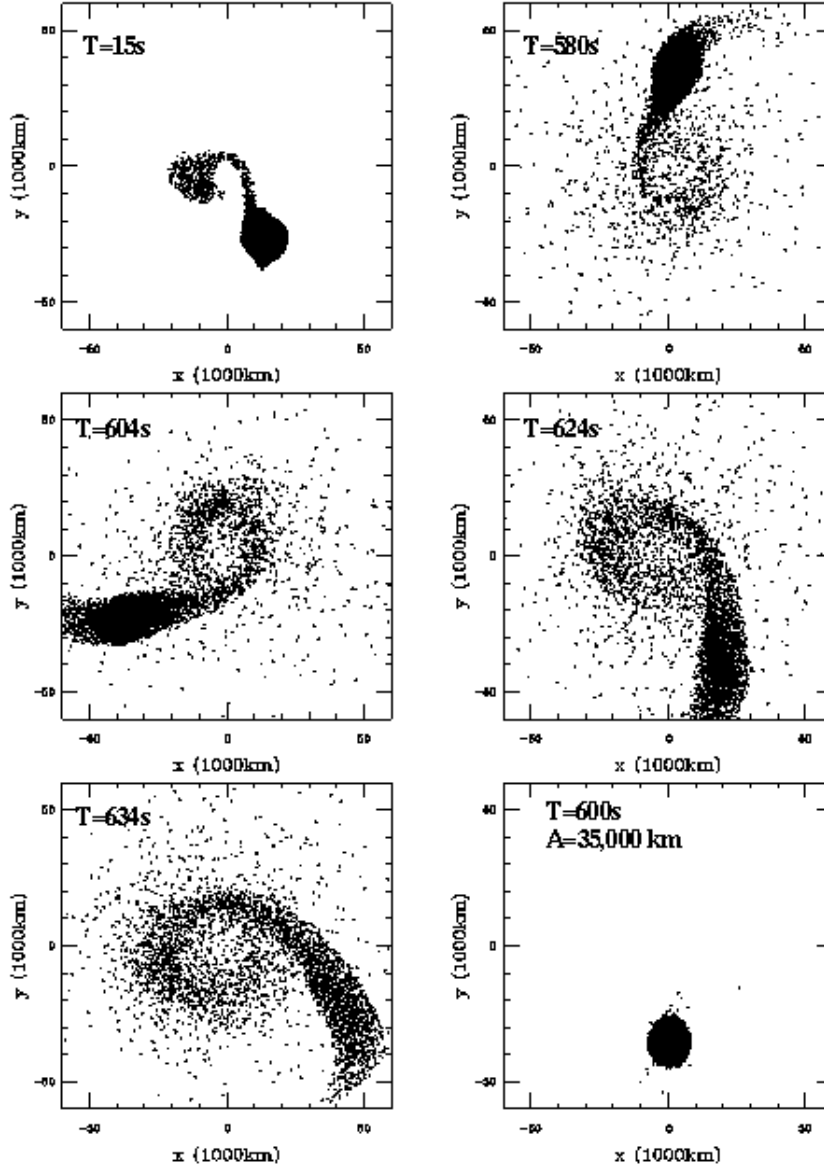


Fig. 3.— Time evolution of a $M_{\text{WD}} = 0.7M_{\odot}$, $M_{\text{BH}} = 3.0M_{\odot}$ simulation. Here we show slices about the z -axis from -10000 - 10000 km. Note that very little accretion occurs for over 600s and then, very rapidly, the white dwarf is torn apart. However, for orbital separations just 20% further out (lower right panel), there is no mass transfer. This suggests our initial conditions are roughly accurate.

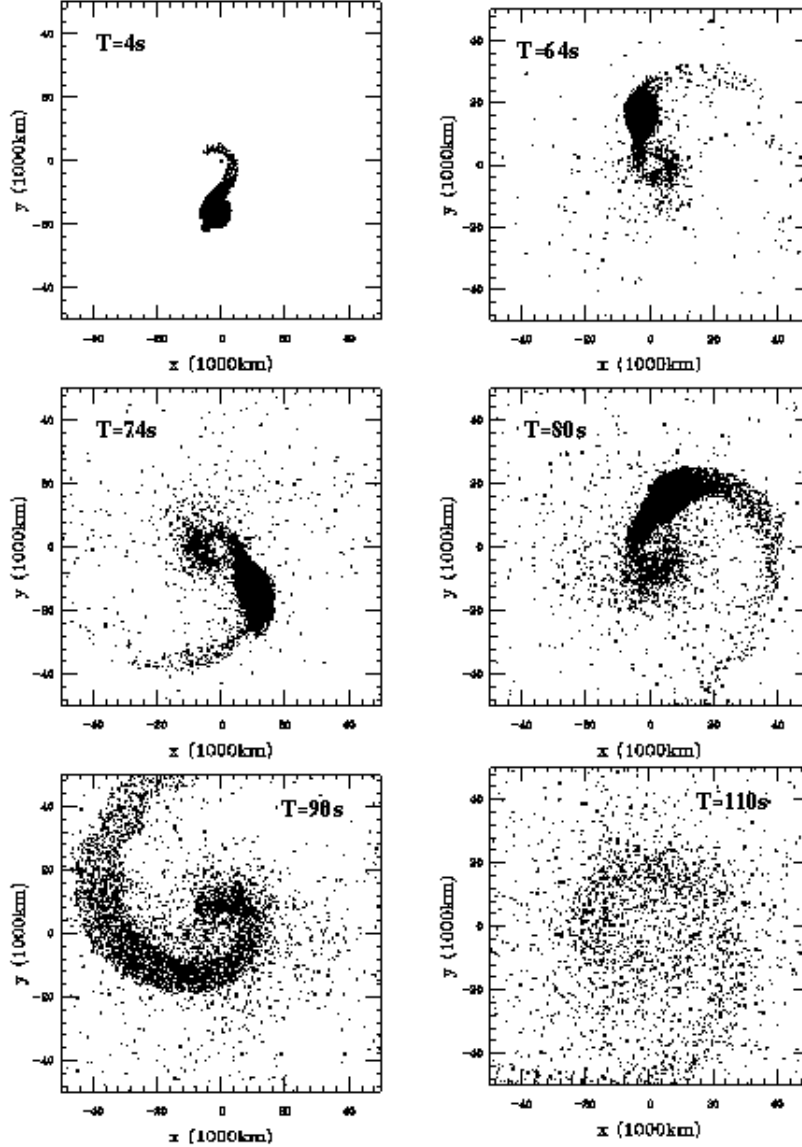


Fig. 4.— Time evolution of a $M_{\text{WD}} = 1.1M_{\odot}$, $M_{\text{BH}} = 3.0M_{\odot}$ simulation. Here we show slices about the z-axis from -10000-10000 km. Note that very little accretion occurs for over 70s and then, very rapidly, the white dwarf is torn apart. In the last slide (T=110s), nearly all traces of the white dwarf have been removed and half of the white dwarf mass has been accreted onto the black hole.

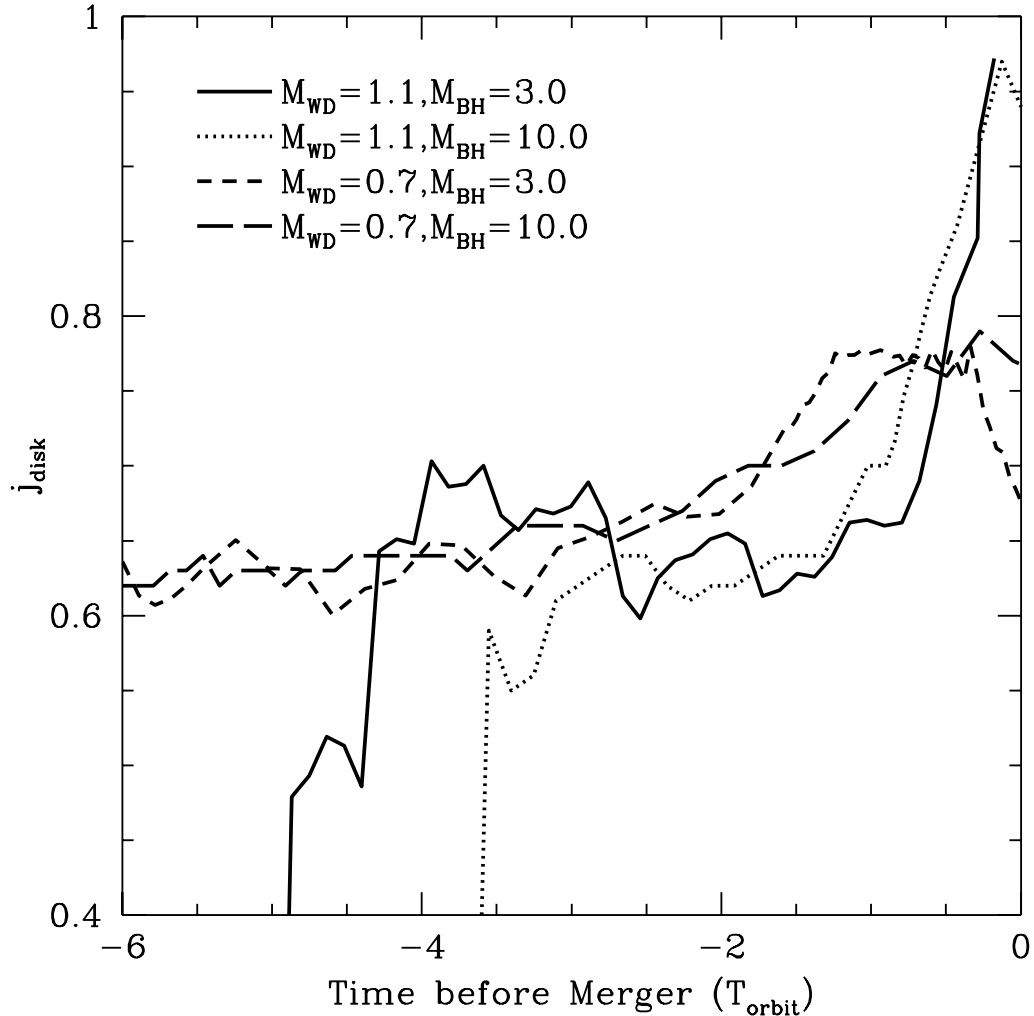


Fig. 5.— The specific angular momentum (j_{disk}) of the disk (in units of the white dwarf specific angular momentum) as a function of time (in orbital time). The orbital times of the systems are given in Table 1. As the white dwarf is disrupted, its entire angular momentum is put in the disk.

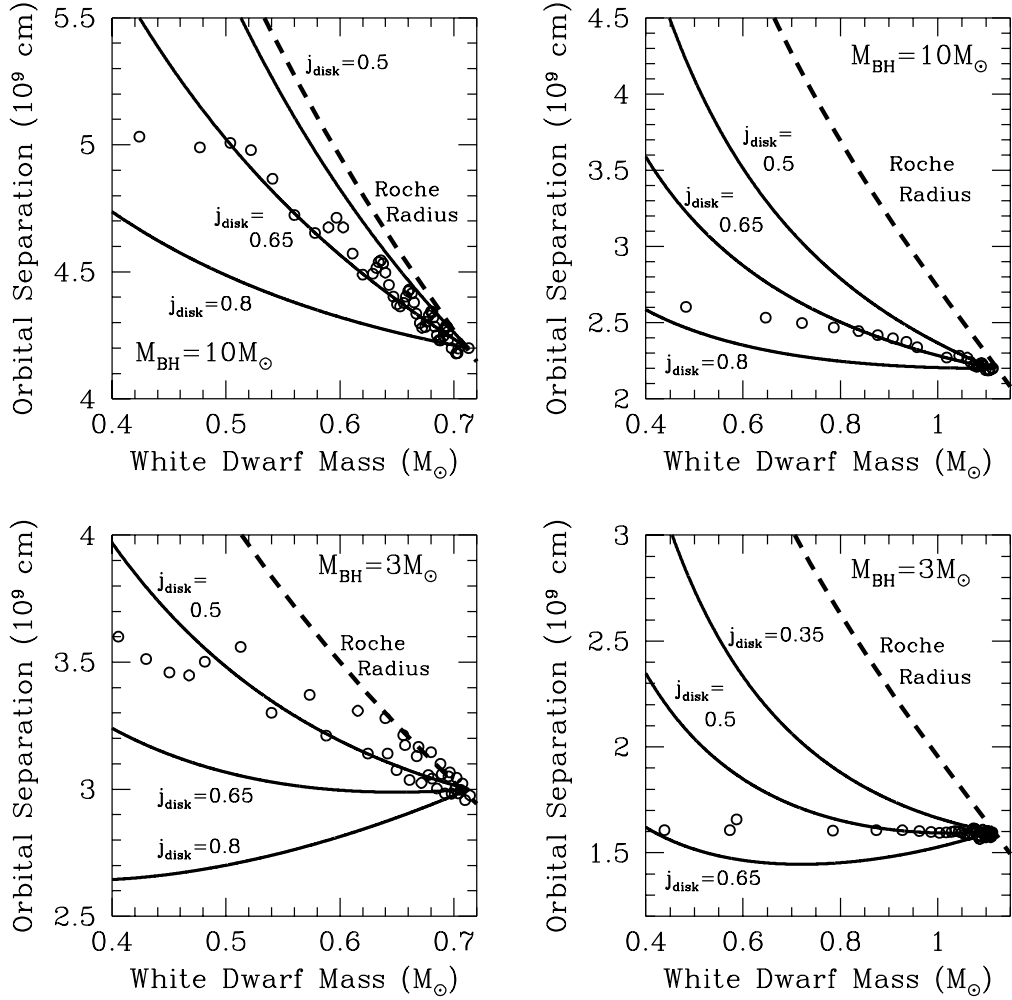


Fig. 6.— Orbital separation as a function of white dwarf mass. The circles are the data from the simulations and the solid lines denote the predicted separations from equation (4). The dashed line is the separation at which the white dwarf overfills its Roche radius. Note that after losing $\sim 0.2M_{\odot}$, the orbital separation evolution remains constant. This occurs as the white dwarf is torn apart by tidal forces.

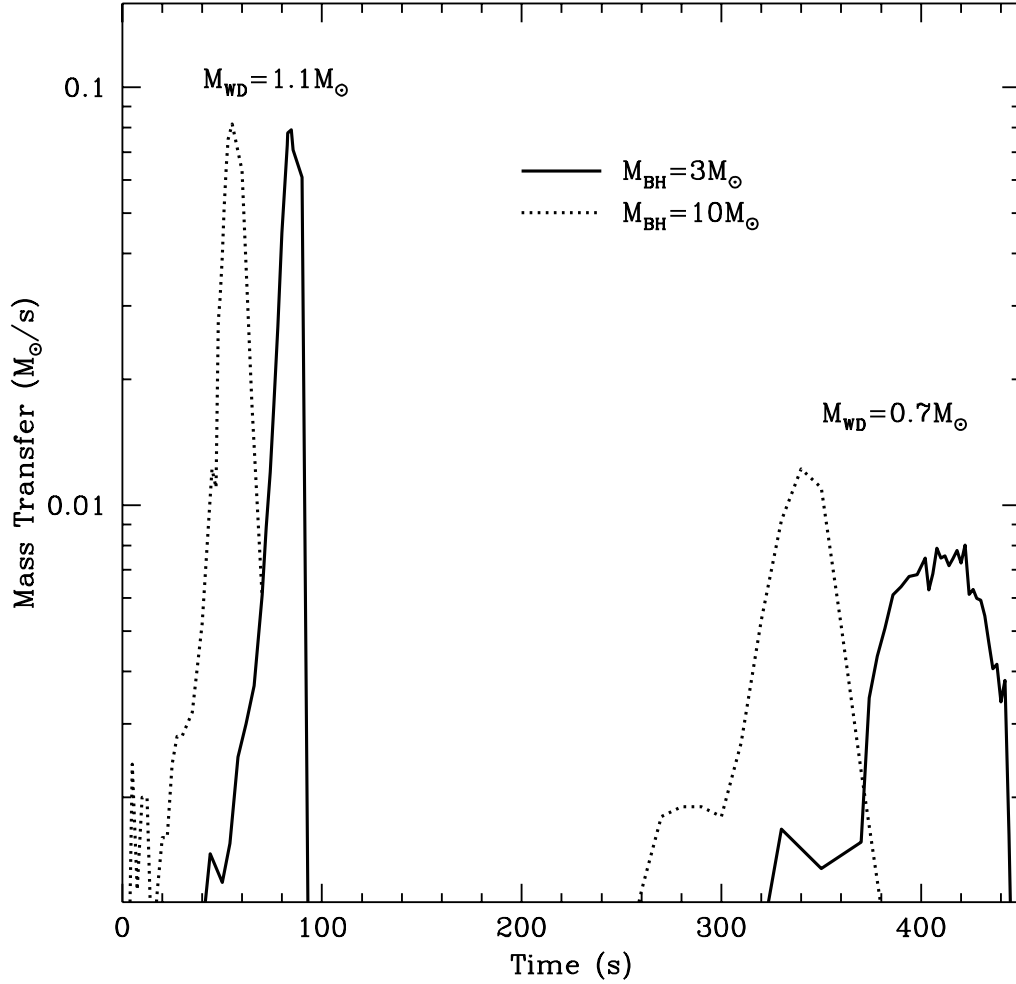


Fig. 7.— Mass Transfer Rate vs. time for the 4 white dwarf/black hole mergers. The more massive white dwarfs merge more quickly and have correspondingly higher mass-transfer rates. This rate gives a maximum for the disk accretion rate onto the black hole.

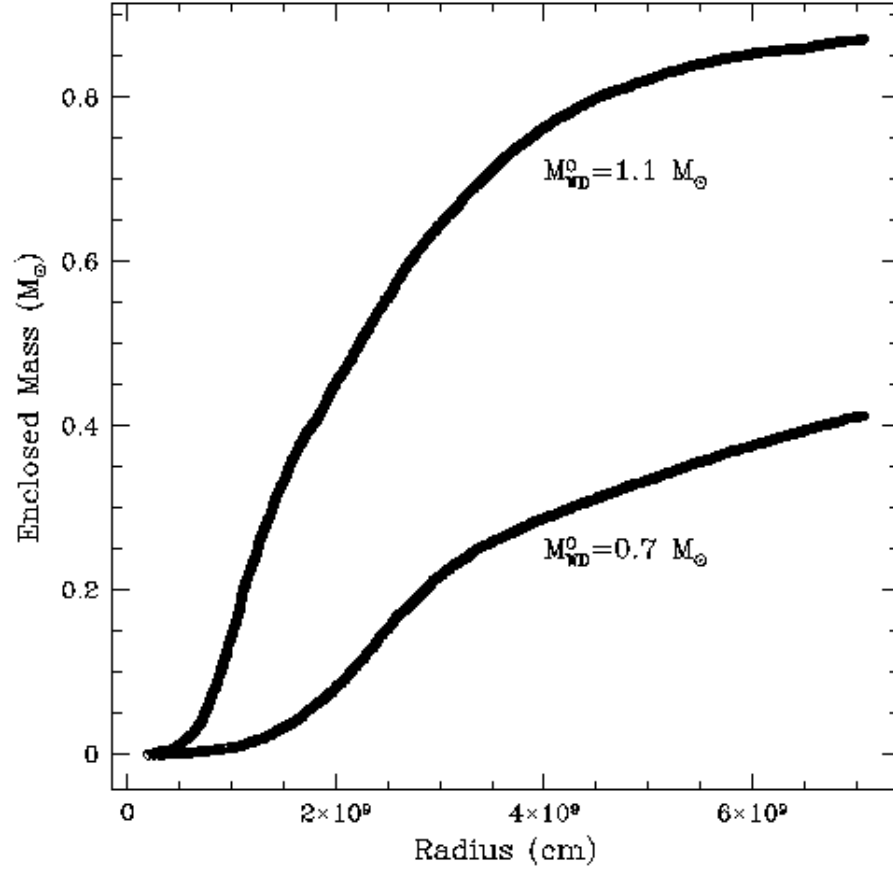


Fig. 8.— Enclosed Mass vs. radius just after white dwarf disruption. The accretion rate of this material onto the disk is roughly given by: $\dot{M}_{\text{acc}} \approx \alpha \Omega M_{\text{disk}}$.

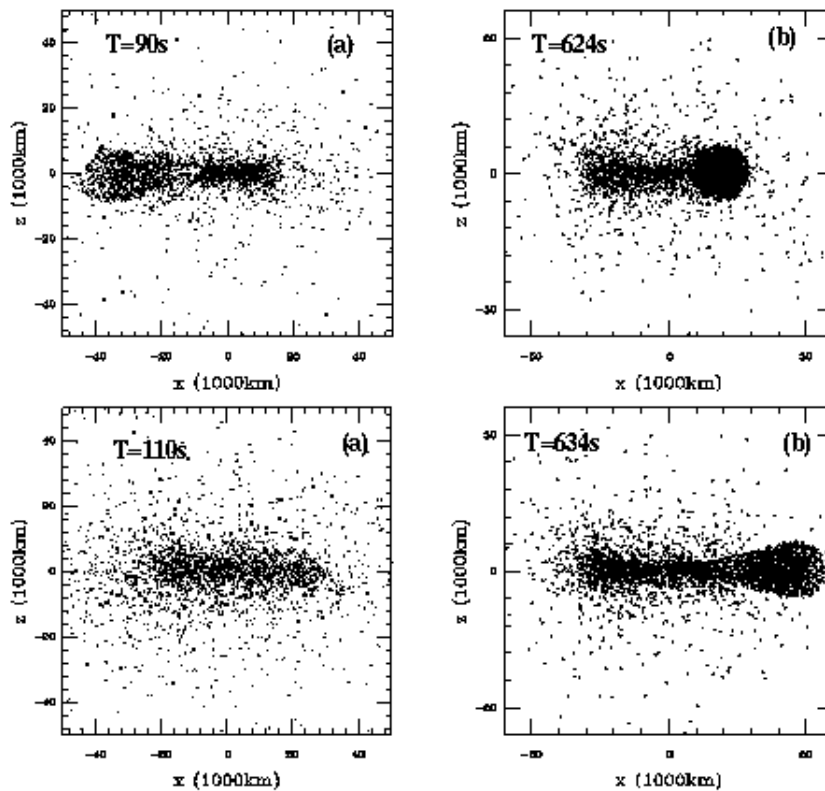


Fig. 9.— Distribution of the white dwarf material along the rotation axis for our two $M_{\text{BH}} = 3M_{\odot}$ simulations. Any GRB explosion must plow through this material (and possibly sweep it up) as it expands. If the explosion is beamed, the total swept up mass is very small (see Table 2) and will not effect the GRB.